Supplementary Information for

Klebsazolicin inhibits 70S ribosome by obstruction of the peptide exit tunnel

Mikhail Metelev[1,2,3,4,*], Ilya A. Osterman[3,5,*], Dmitry Ghilarov[3,4], Nelli F. Khabibullina[6], Alexander Yakimov[1,7], Konstantin Shabalin[7], Irina Utkina[1,3], Dmitry Y. Travin[8], Ekaterina S. Komarova[8], Marina Serebryakova[4,5], Tatyana Artamonova[1], Mikhail Khodorkovskii[1], Andrey L. Konevega[1,7], Petr V. Sergiev[3,5], Konstantin Severinov[1,3,4,9,†], and Yury S. Polikanov[6,10,†]

[1] Research Center of Nanobiotechnologies, Peter the Great St.Petersburg Polytechnic University, Saint-Petersburg, 195251, Russia
[2] Institute of Antimicrobial Chemotherapy, Smolensk State Medical Academy, Smolensk, 214018, Russia
[3] Skolkovo Institute of Science and Technology, Moscow, 143025, Russia
[4] Institute of Gene Biology of the Russian Academy of Sciences, Moscow, 119334, Russia
[5] Lomonosov Moscow State University, Department of Chemistry and A.N. Belozersky Institute of Physico-Chemical Biology, Moscow, 119992, Russia
[6] Department of Biological Sciences, University of Illinois at Chicago, Chicago, IL 60607, USA
[7] Petersburg Nuclear Physics Institute, NRC "Kurchatov Institute", Gatchina, 188300, Russia
[8] Lomonosov Moscow State University, Department of Bioengineering and Bioinformatics, Moscow, 119992, Russia
[9] Waksman Institute for Microbiology, Rutgers, The State University of New Jersey, Piscataway, NJ 08854, USA
[10] Department of Medicinal Chemistry and Pharmacognosy, University of Illinois at Chicago, Chicago, IL 60607, USA

* Authors contributed equally to this work
† To whom correspondence should be addressed.
E-mail: yuryp@uic.edu (Y.S.P.)
severik@waksman.rutgers.edu (K.S.)

This file includes:

SUPPLEMENTARY RESULTS

I. SUPPLEMENTARY FIGURES

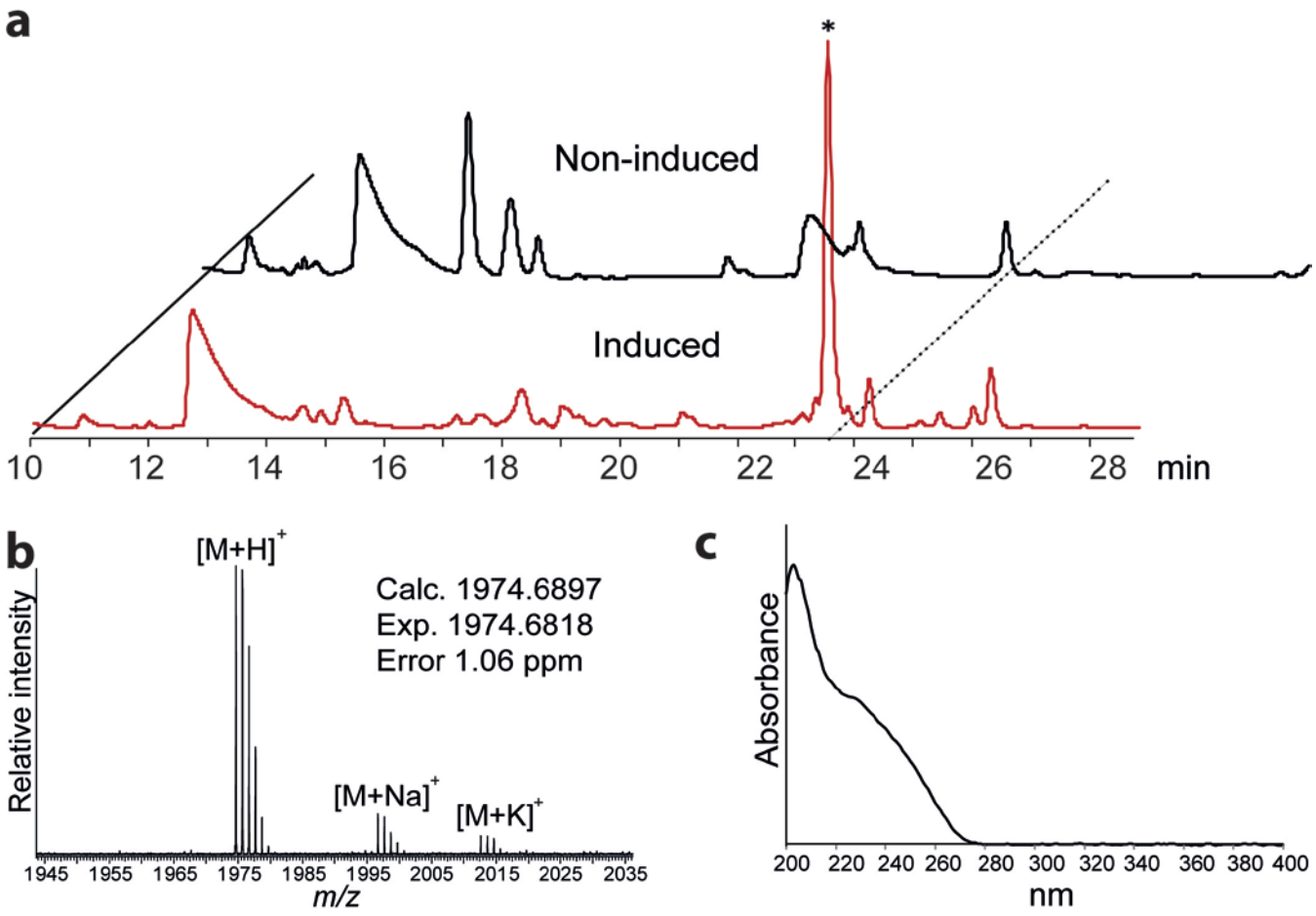

Supplementary Figure 1 | Production of klebsazolicin by *E. coli* host. (**a**) Comparison of HPLC-UV traces of supernatants of non-induced (black) and induced (red) cultures of *E. coli* cells carrying the *klpABCDE* gene cluster. KLB-containing fraction is labeled by an asterisk. (**b**) FT-MS spectra of HPLC-purified KLB. The *m/z* values of major peak $[M+H]^+$ as well as $[M+Na]^+$ and $[M+K]^+$ are indicated. Experimentally measured and calculated values of *m/z* $[M+H]^+$ are indicated. (**c**) UV-Vis absorption spectrum of HPLC-purified KLB. Note that KLB displays absorbance that is characteristic for azole-containing peptides.

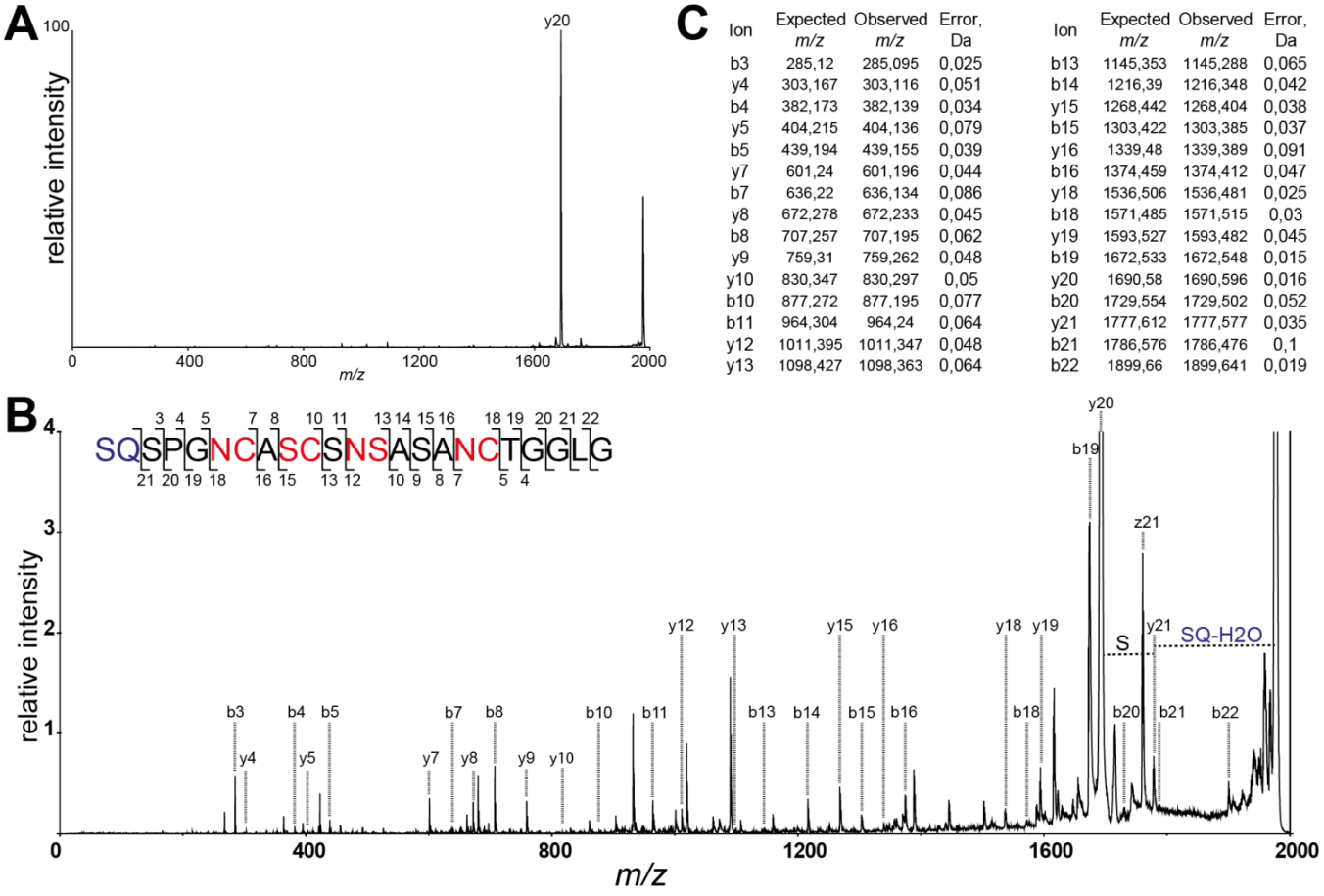

C

Ion	Expected *m/z*	Observed *m/z*	Error, Da	Ion	Expected *m/z*	Observed *m/z*	Error, Da
b3	285,12	285,095	0,025	b13	1145,353	1145,288	0,065
y4	303,167	303,116	0,051	b14	1216,39	1216,348	0,042
b4	382,173	382,139	0,034	y15	1268,442	1268,404	0,038
y5	404,215	404,136	0,079	b15	1303,422	1303,385	0,037
b5	439,194	439,155	0,039	y16	1339,48	1339,389	0,091
y7	601,24	601,196	0,044	b16	1374,459	1374,412	0,047
b7	636,22	636,134	0,086	y18	1536,506	1536,481	0,025
y8	672,278	672,233	0,045	b18	1571,485	1571,515	0,03
b8	707,257	707,195	0,062	y19	1593,527	1593,482	0,045
y9	759,31	759,262	0,048	b19	1672,533	1672,548	0,015
y10	830,347	830,297	0,05	y20	1690,58	1690,596	0,016
b10	877,272	877,195	0,077	b20	1729,554	1729,502	0,052
b11	964,304	964,24	0,064	y21	1777,612	1777,577	0,035
y12	1011,395	1011,347	0,048	b21	1786,576	1786,476	0,1
y13	1098,427	1098,363	0,064	b22	1899,66	1899,641	0,019

Supplementary Figure 2 | MS/MS fragmentation analysis of klebsazolicin. (**a**) MALDI-TOF-MS analysis of purified KLB resulted in identification of ion consistent with the calculated *m/z* of KLB. The ion was fragmented and produced represented spectrum with the predominant fragmentation between Ser3 and Pro4. (**b**) Zoomed MS-MS spectrum and the diagram of KLB with the observed *b*- and *y*-ions labeled in the structure and in the spectra. (**c**) Expected *m/z*, observed *m/z*, and error are shown for *b*- and *y*-ions present in the spectrum.

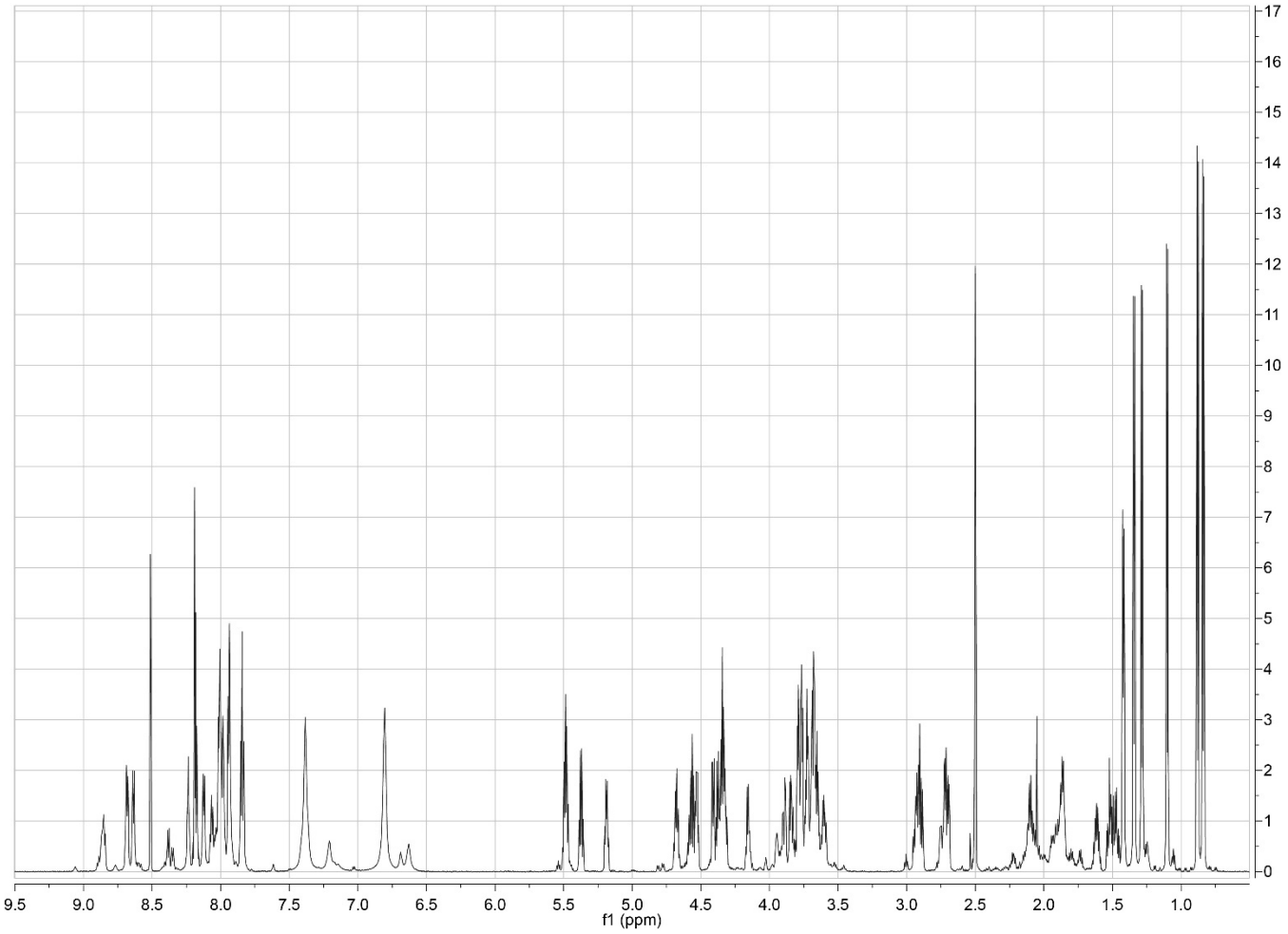

Supplementary Figure 3a | 1H spectrum of klebsazolicin in DMSO-d6 solvent.

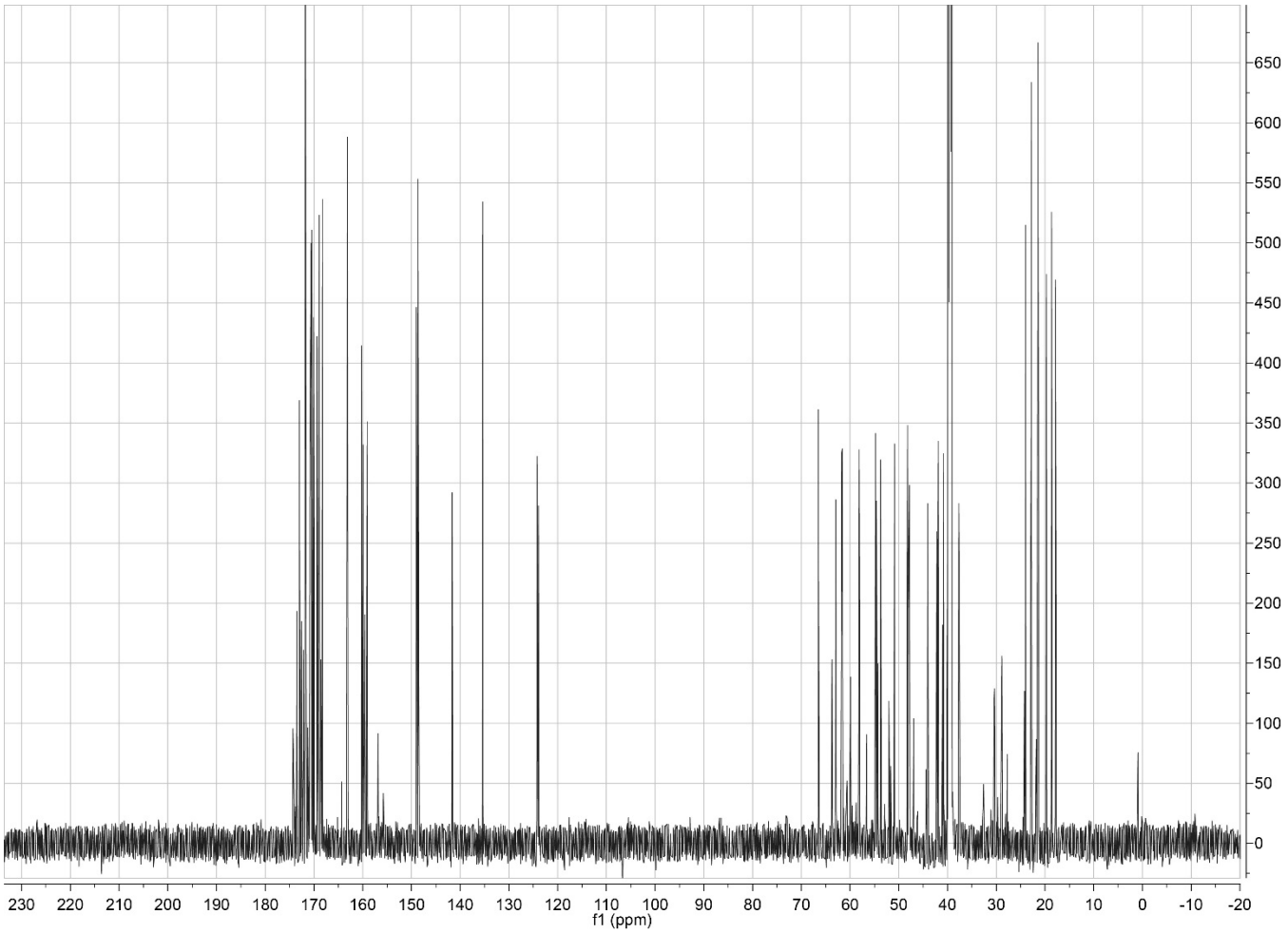

Supplementary Figure 3b | 13C spectrum of klebsazolicin in DMSO-d6 solvent.

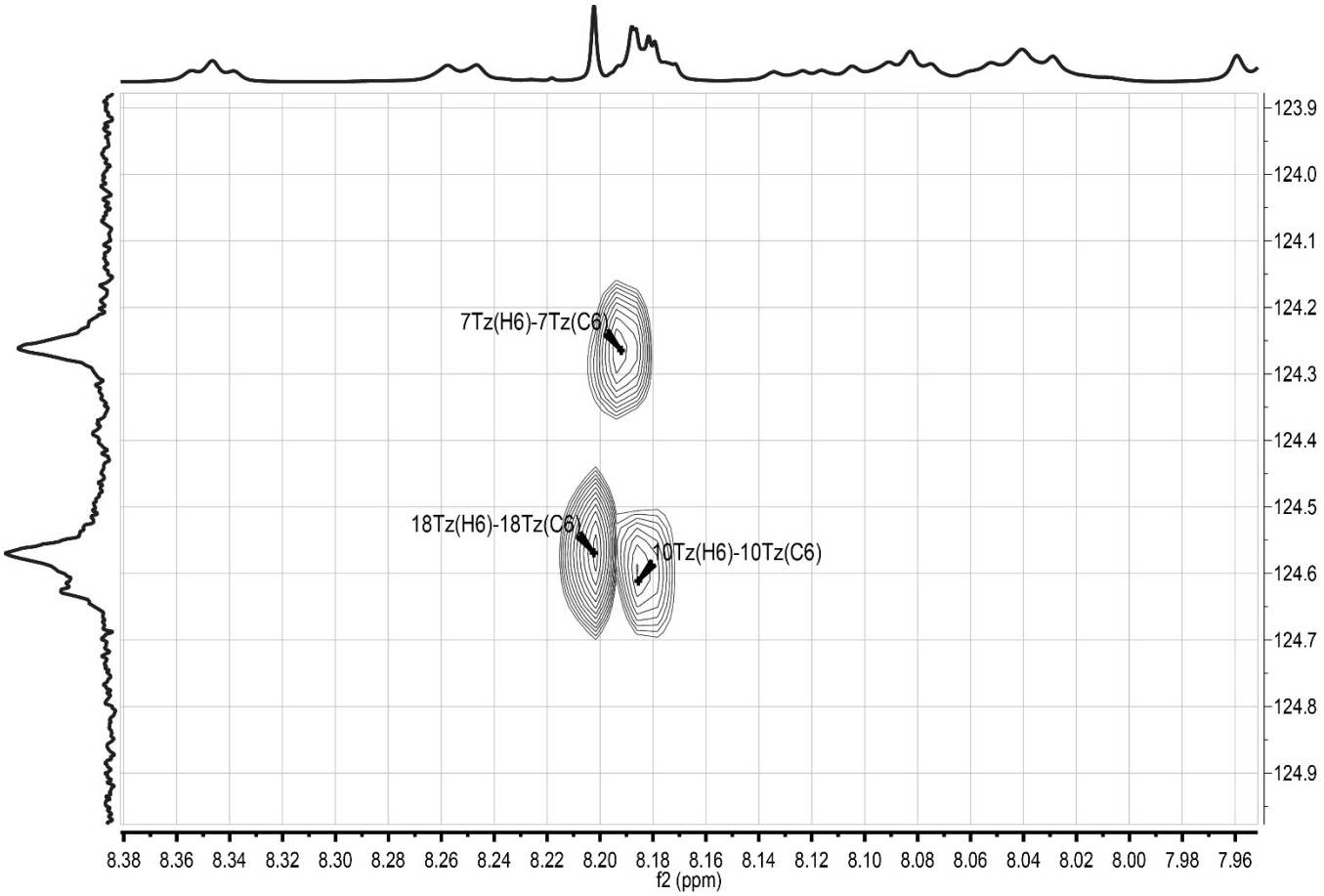

Supplementary Figure 3c | Fragments of the 13C-HSQC spectrum with assignments of thiazoles.

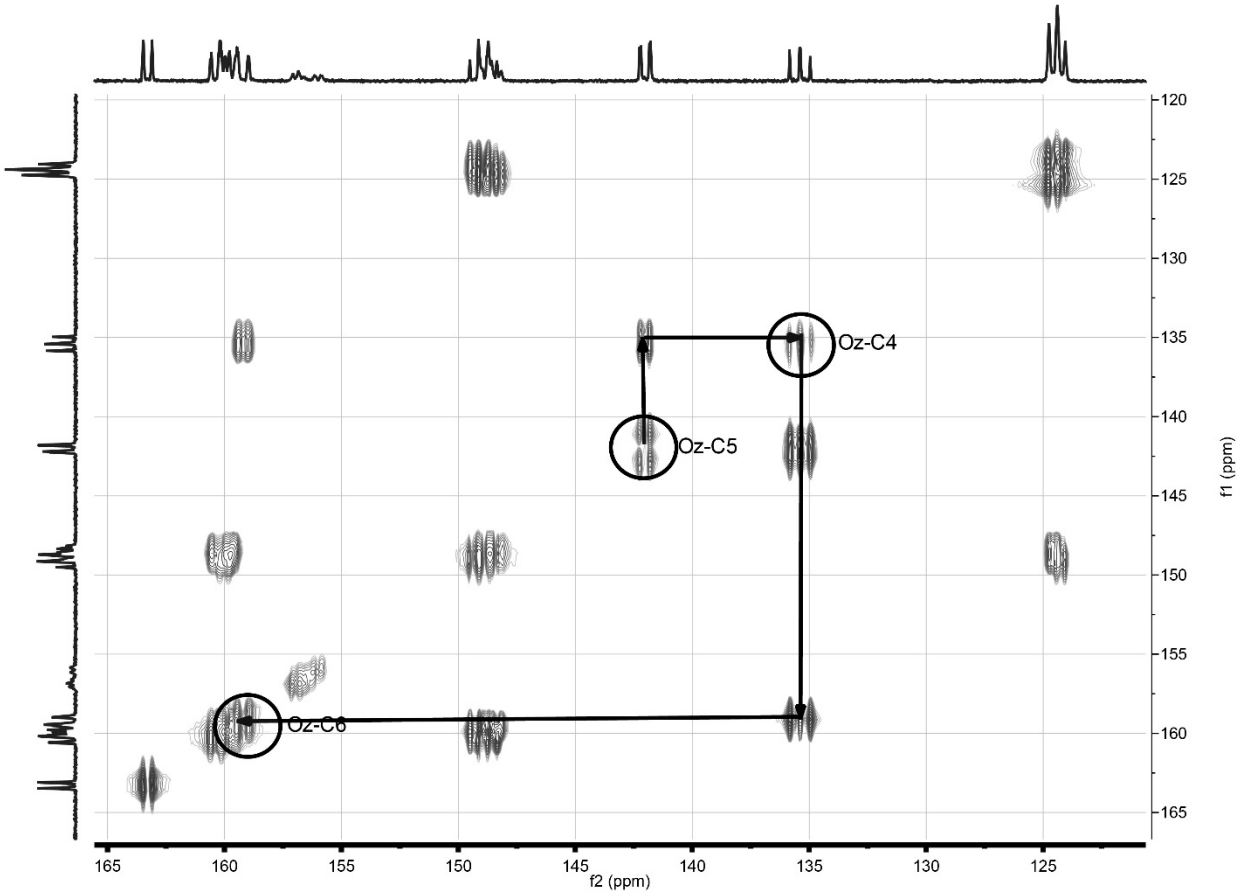

Supplementary Figure 3d | Fragments of the 13C-COSY spectrum with assignment of oxazole.

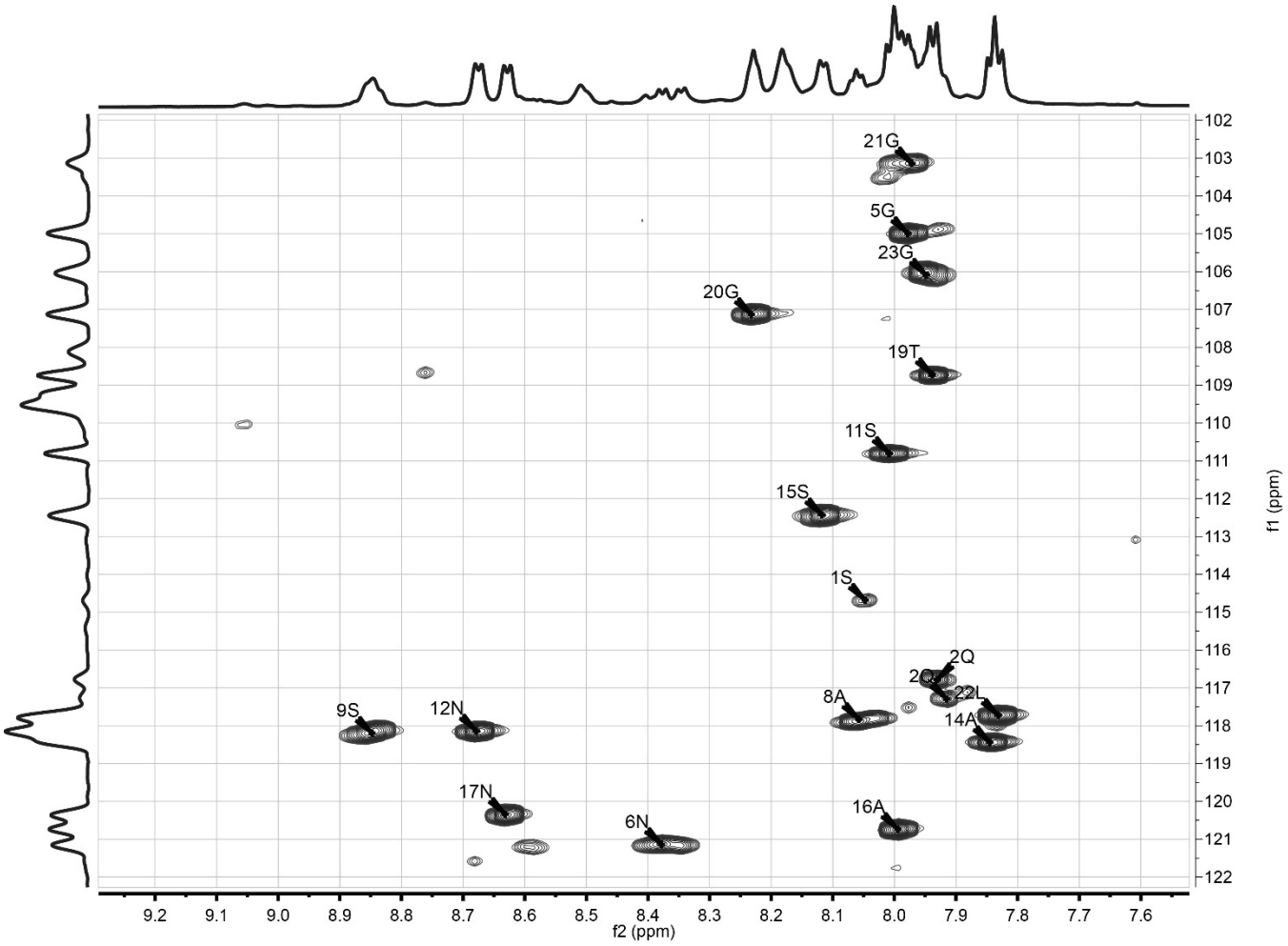

Supplementary Figure 3e | Amide region of the 1H-15N HSQC spectra of KLB.

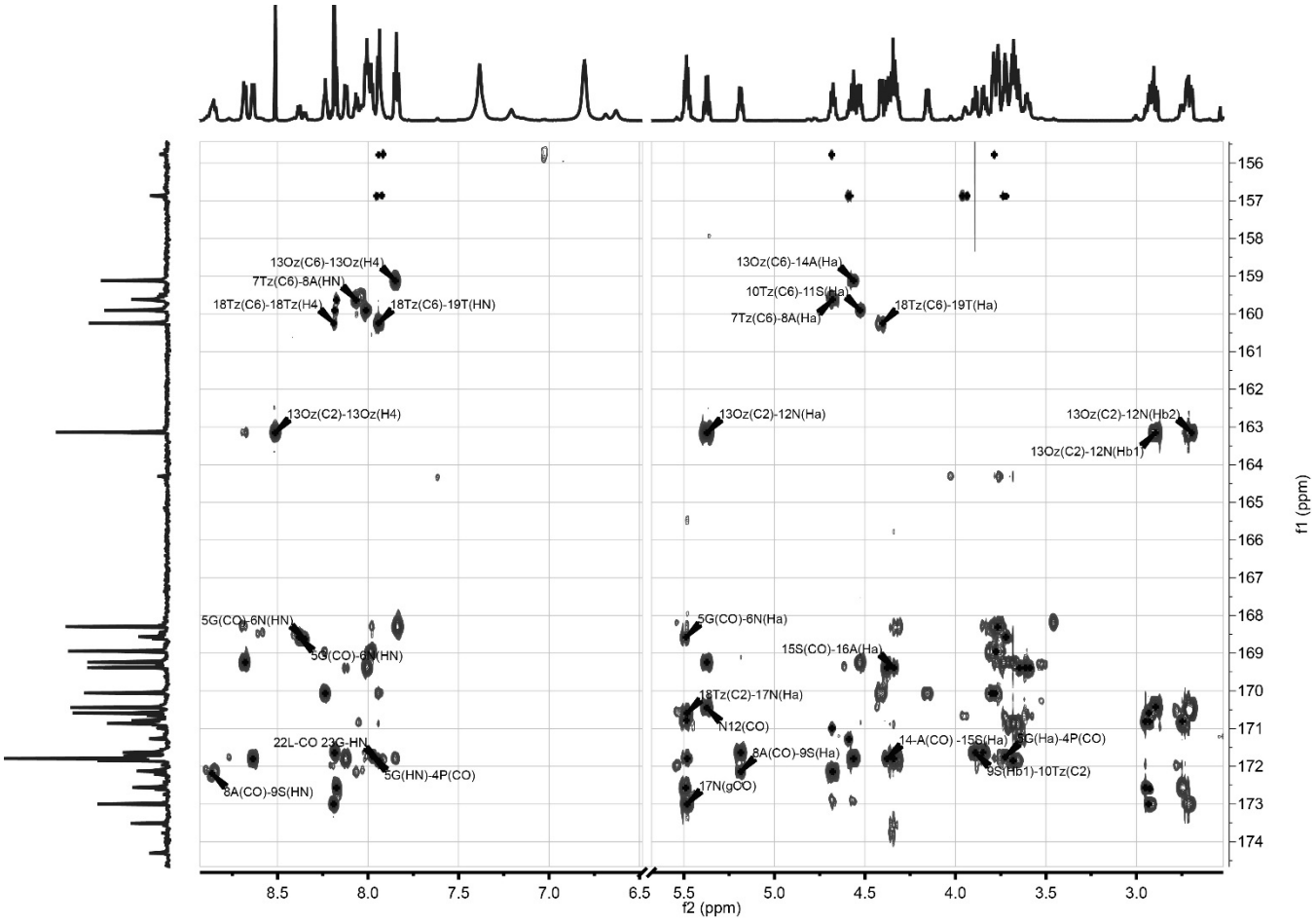

Supplementary Figure 3f | Fragments of the 13C-HMBC spectrum.

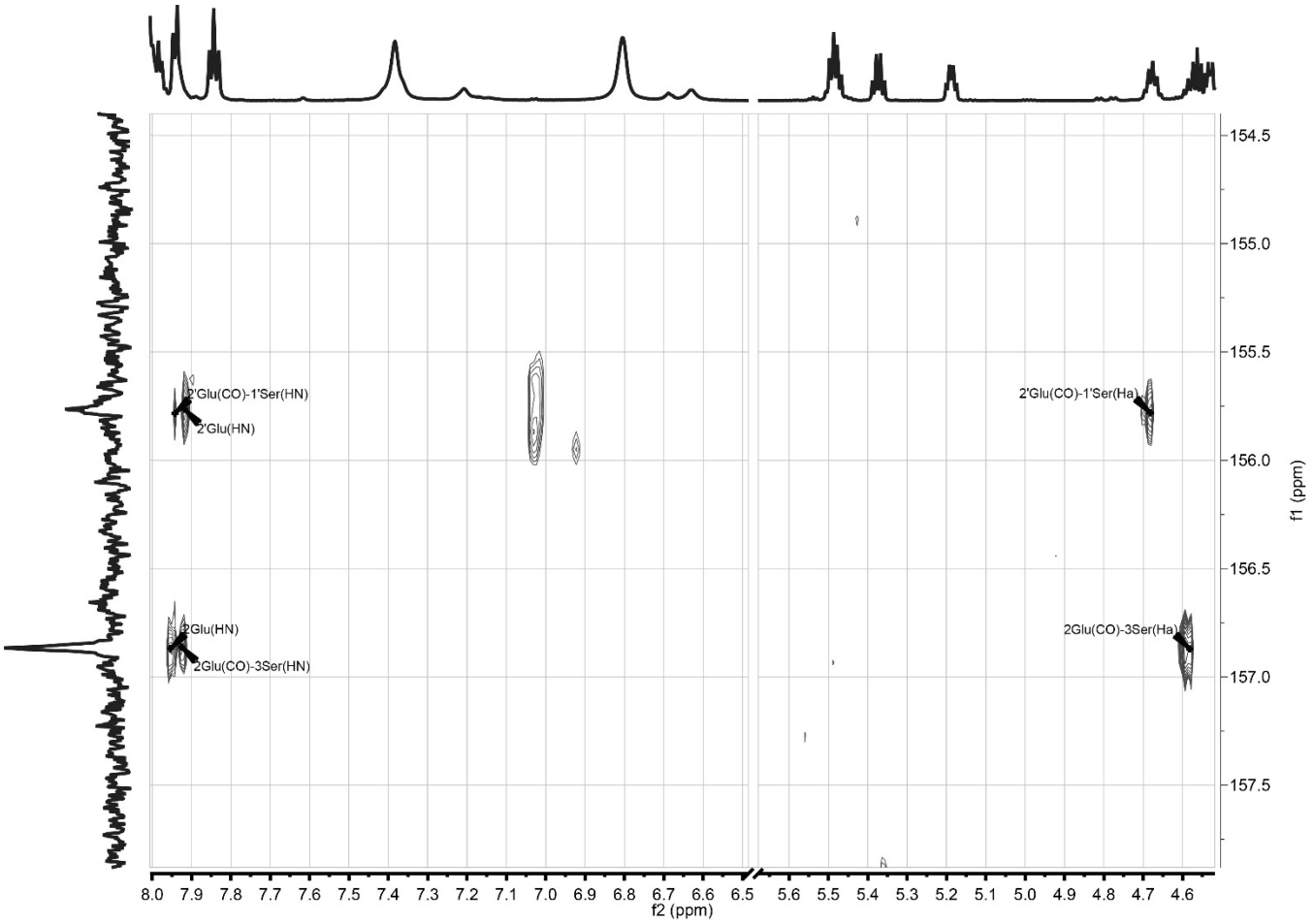

Supplementary Figure 3g | Fragments of the 13C-HMBC spectrum (Ser1, Glu2 and Ser3).

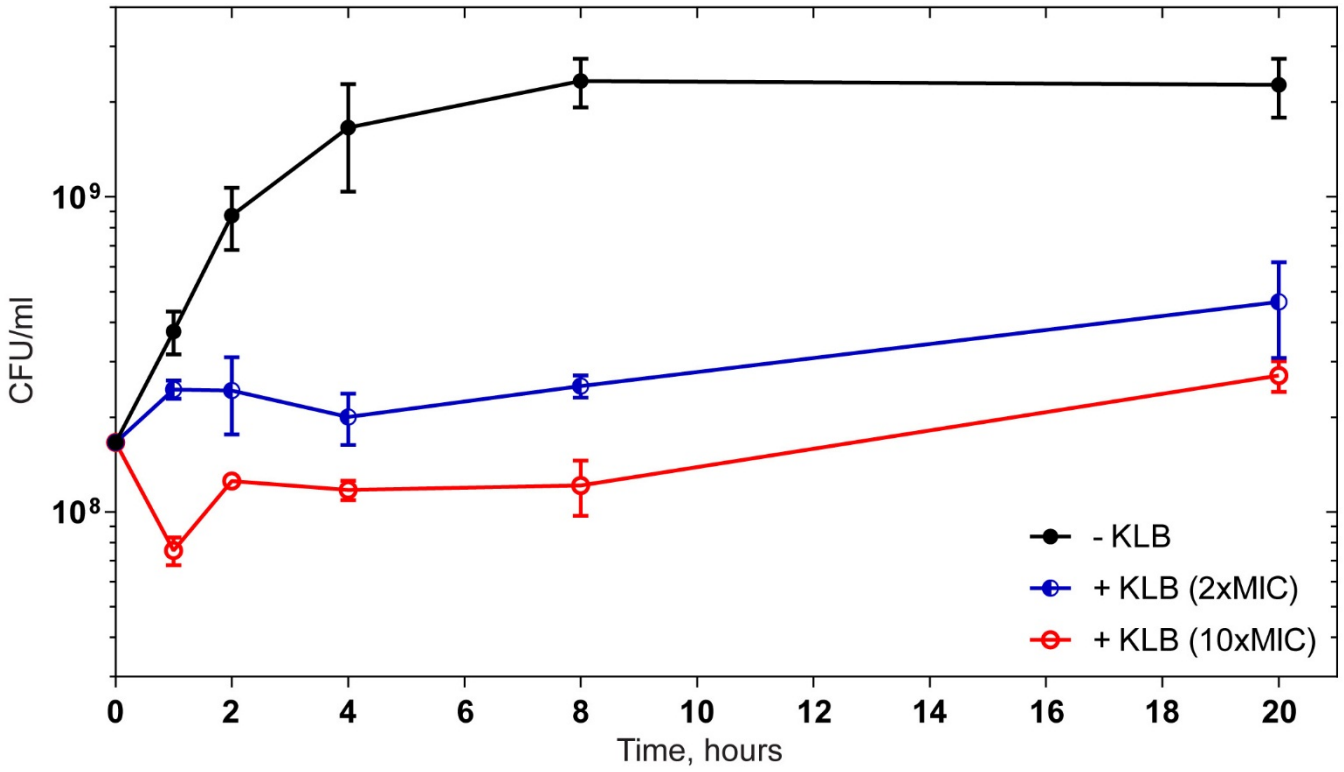

Supplementary Figure 4 | Klebsazolicin displays bacteriostatic activity. Exponentially growing cultures of *E. coli* B cells were exposed to 0, 2-fold MIC (4μM), and 10-fold MIC (20 μM) KLB. Cells were grown in M9 medium supplemented with 0.4% glucose. The numbers of survived cells were determined by plating on solid LB plates. Each point represent average of three experiments for each culture, error bars indicate standard deviations.

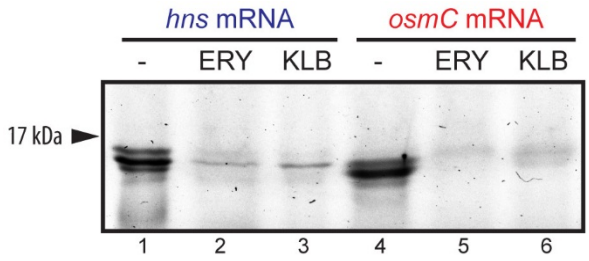

Supplementary Figure 5 | Inhibition of full-length product accumulation on *hns* and *osmC* mRNAs by erythromycin (ERY) and klebsazolicin (KLB). *hns* and *osmC* mRNAs were obtained by transcription with T7 RNA-polymerase, and then used for *in vitro* translation in S30 *E. coli* extract in the presence of fluorescently labeled lysine. The products were separated by SDS-PAGE and visualized by Typhoon FLA 9500. The concentrations of erythromycin and klebsazolicin both were 5 μM.

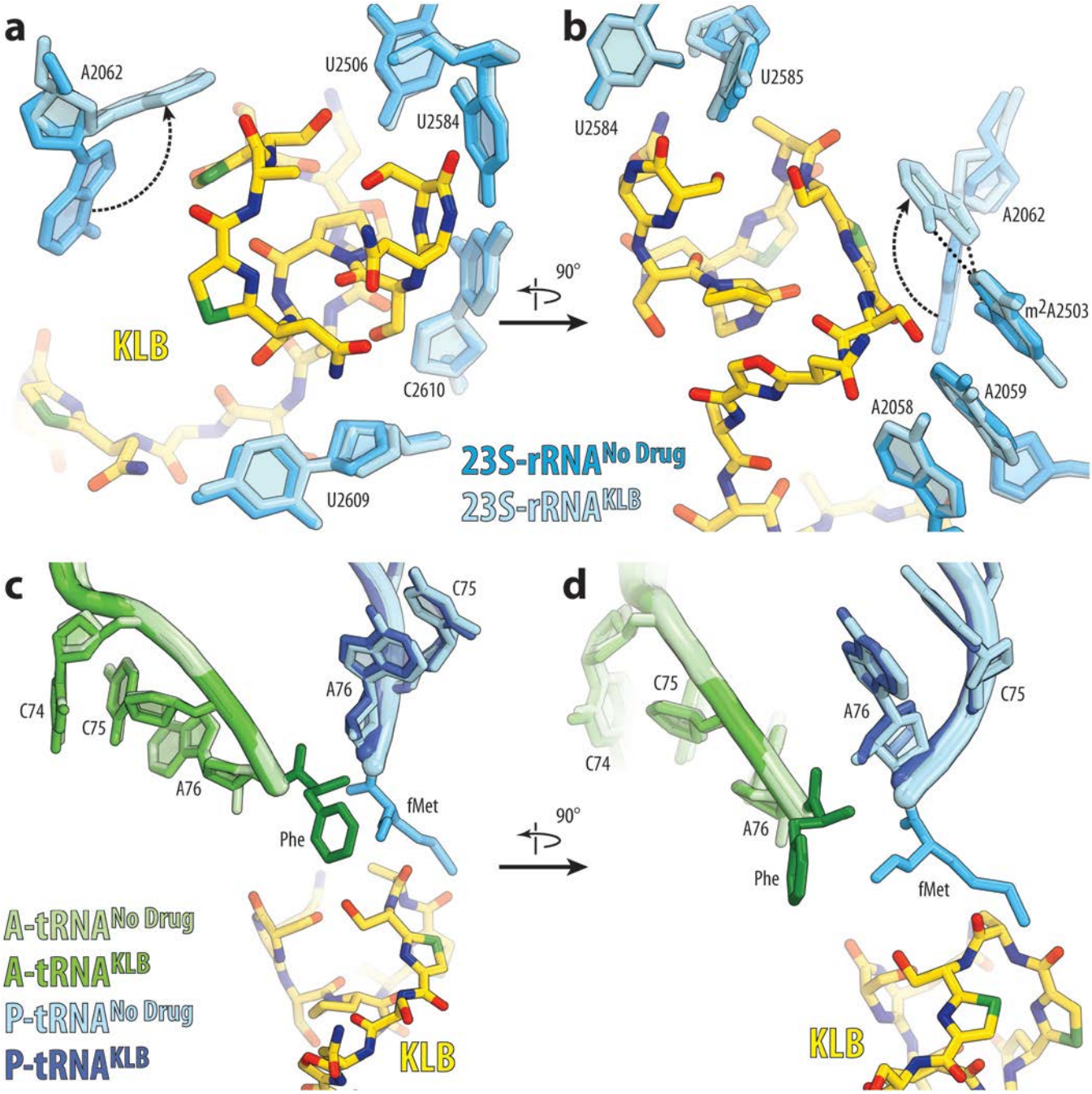

Supplementary Figure 6 | Effects of KLB binding on the conformations of the nucleotides in the 23S rRNA. (**a, b**) Comparison of the positions of key nucleotides in the 23S rRNA around the PTC in the presence of KLB (light blue) and in the canonical pre-attack state (blue) without the drug viewed from two different orientations. The structure coordinates for the position of the aminoacylated tRNAs in the pre-attack state are from the PDB entry 1VY4[1]. Note that the only nucleotide in the 23S rRNA whose conformation significantly changes upon binding of KLB is A2602, which rotates by more than ninety degrees to form Hoogsteen base-pair with the m^2A2503. (**c, d**) Comparison of the positions of the CCA-

ends of the A- and P-site tRNAs in the presence of KLB (green and dark blue, respectively) and its absence with the canonical positions of the aminoacylated tRNAs. For reference, the fully accommodated tRNA in the A site (light green with the Phe moiety shown in dark green) and the P-site tRNA (light blue with the fMet moiety colored in blue) are shown from two different views. The structure coordinates for the position of the aminoacylated tRNAs in the pre-attack state are from the PDB entry 1VY4[1]. Note that presence of KLB does not affect positioning of the CCA-ends of the tRNAs in the PTC.

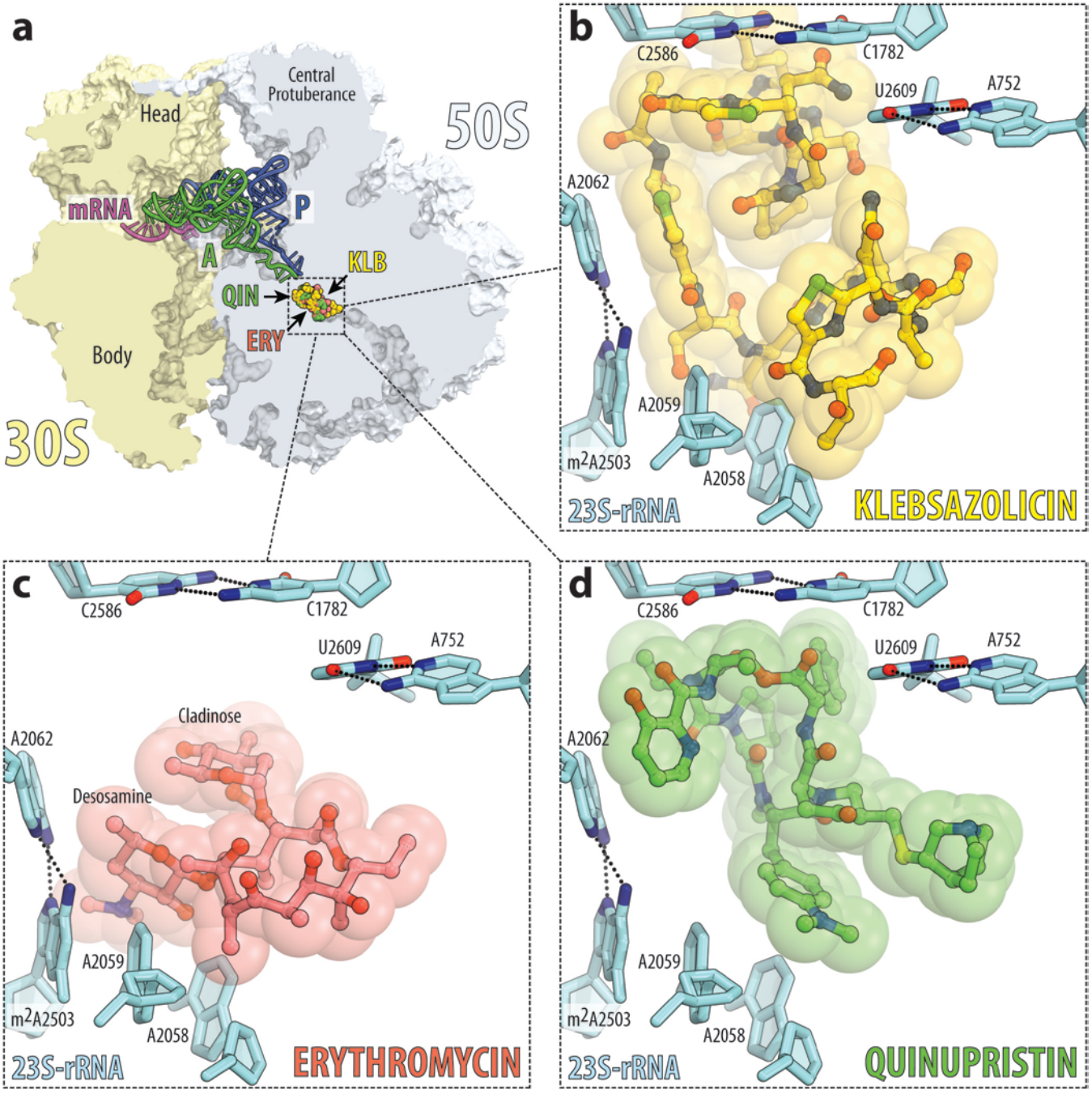

Supplementary Figure 7 | Comparison of the binding sites of antibiotics in the peptidyl transferase center. (**a**) Overview of the superimposed binding sites of klebsazolicin (KLB, yellow), erythromycin (ERY, light red), and quinupristin (QIN, green) in the PTC of the 50S subunit. The view and the coloring of 23S rRNA, mRNA and tRNAs are the same as in Fig. 4. KLB structure is from the current work, ERY is from PDB entry 4V7X[2], and QIN is from PDB entry 4U26[3]. All structures were aligned based on the domain V of the 23S rRNA. (**b**, **c**, **d**) Close-up views of the binding sites shown in (a) for KLB, ERY, and

QIN respectively. Note that macrolides (ERY) or streptogramins B (QIN) only partially occlude the peptide exit tunnel, whereas klebsazolicin (KLB) significantly obstructs it.

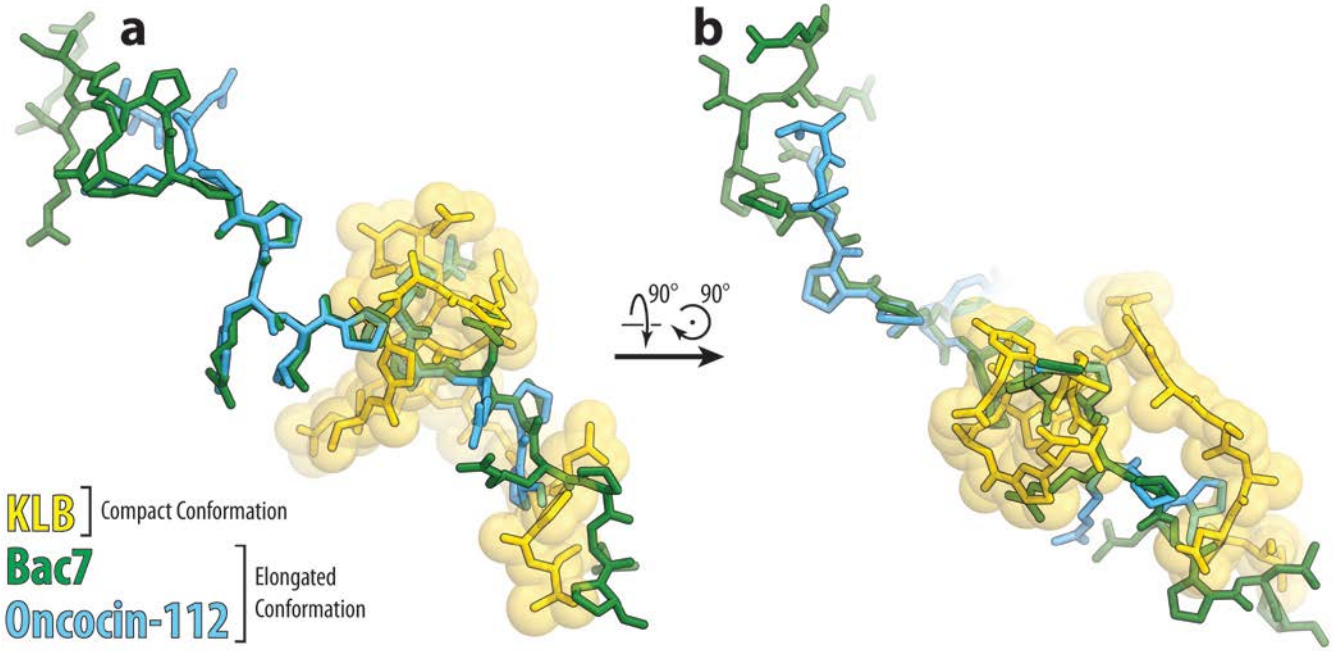

Supplementary Figure 8 | Superposition of 70S-KLB structure with the ribosome-bound translation inhibitor peptides Oncocin and Bac7. (**a, b**) Close-up views of the structure of KLB (yellow) in complex with the *T. thermophilus* 70S ribosome superimposed with the structure of ribosome-bound Bac7 peptide (green) (PDB entry 5HAU [4]) and Oncocin-112 peptide (PDB entry 4Z8C [5]). Superposition is based on the alignment of the 23S rRNA. Subunits of the 70S ribosome, mRNA and tRNAs are omitted for clarity). Note that Bac7 and Oncocin bind to the ribosomal peptide exit tunnel in the elongated conformation, while KLB binds in a compact globular conformation.

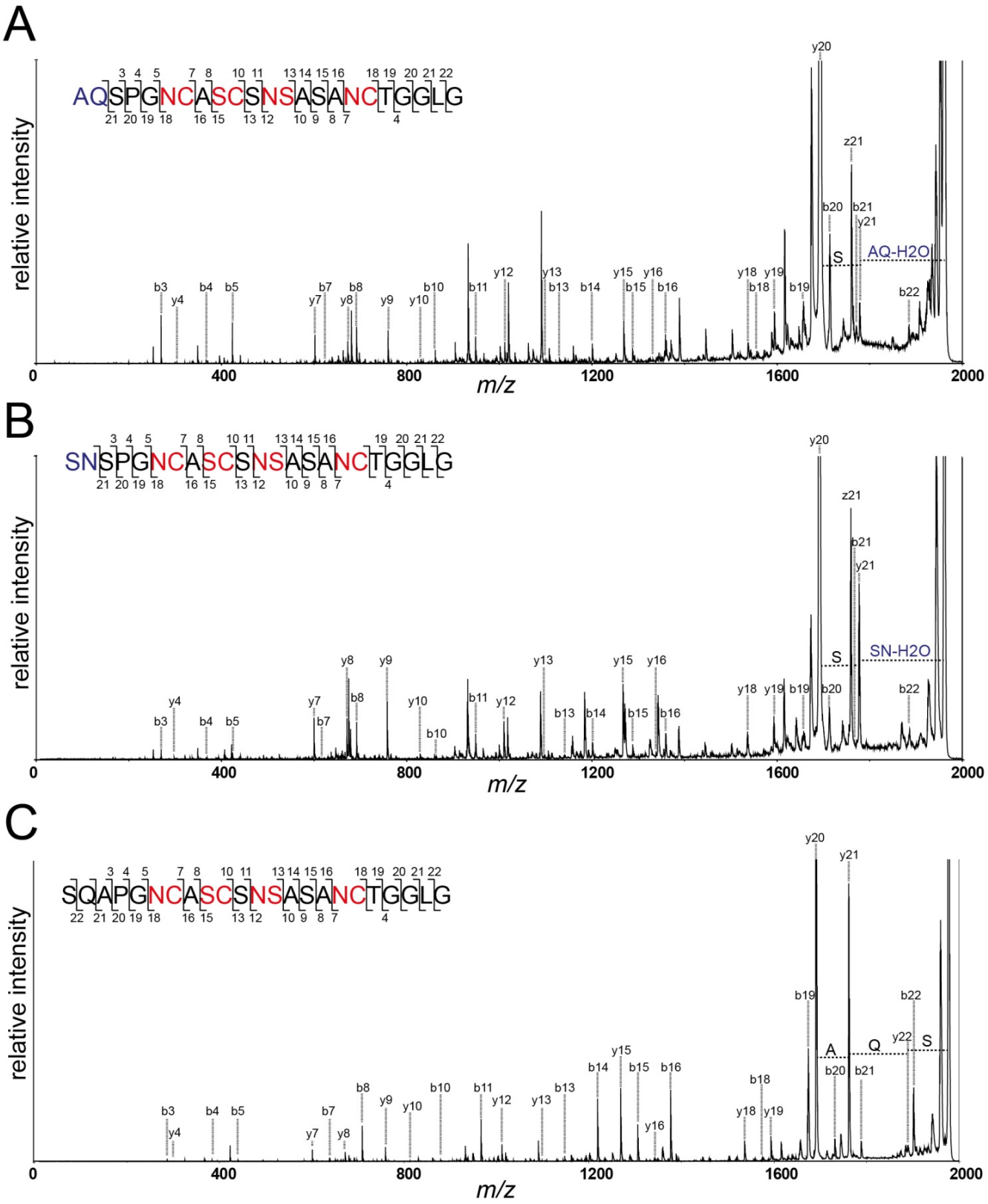

Supplementary Figure 9 | MS/MS fragmentation spectrum of KLB^{S1A}, KLB^{Q2N}, and KLB^{S3A}. (**a**) An *m/z* scan of purified KLB^{S1A} derivative resulted in ion consistent with the calculated *m/z* of for KLB^{S3A}

with amidine ring (observed $[M+H]^+$ at *m/z* 1958.6929, calculated $[M+H]^+$ 1958.6968, Δppm=1.99). The ion was fragmented and produced represented spectra. The diagram of KLB^{S1A} with the observed *b*- and *y*-ions labeled in the structure and in the spectra. (**b**) An *m/z* scan of purified KLB^{Q2N} derivative resulted in ion consistent with the calculated *m/z* of for KLB^{Q2N} with amidine ring (observed $[M+H]^+$ at *m/z* 1960.6693, calculated $[M+H]^+$ 1960.6761, Δppm=3.47). The ion was fragmented and produced represented spectra. The diagram of KLB^{Q2N} with the observed *b*- and *y*-ions labeled in the structure and in the spectra. **(c)** An *m/z* scan of purified KLB^{S3A} derivative resulted in ion consistent with the calculated *m/z* of for KLB^{S3A} that doesn't contain an amidine ring (observed $[M+H]^+$ at *m/z* 1976.7048, calculated $[M+H]^+$ 1976.7074, Δppm=1.32). The ion was fragmented and produced represented spectra. The diagram of KLB^{S3A} with the observed *b*- and *y*-ions labeled in the structure and in the spectra. Presence of y_{22}-ion and no loss of H2O molecule support the absence of amidine ring.

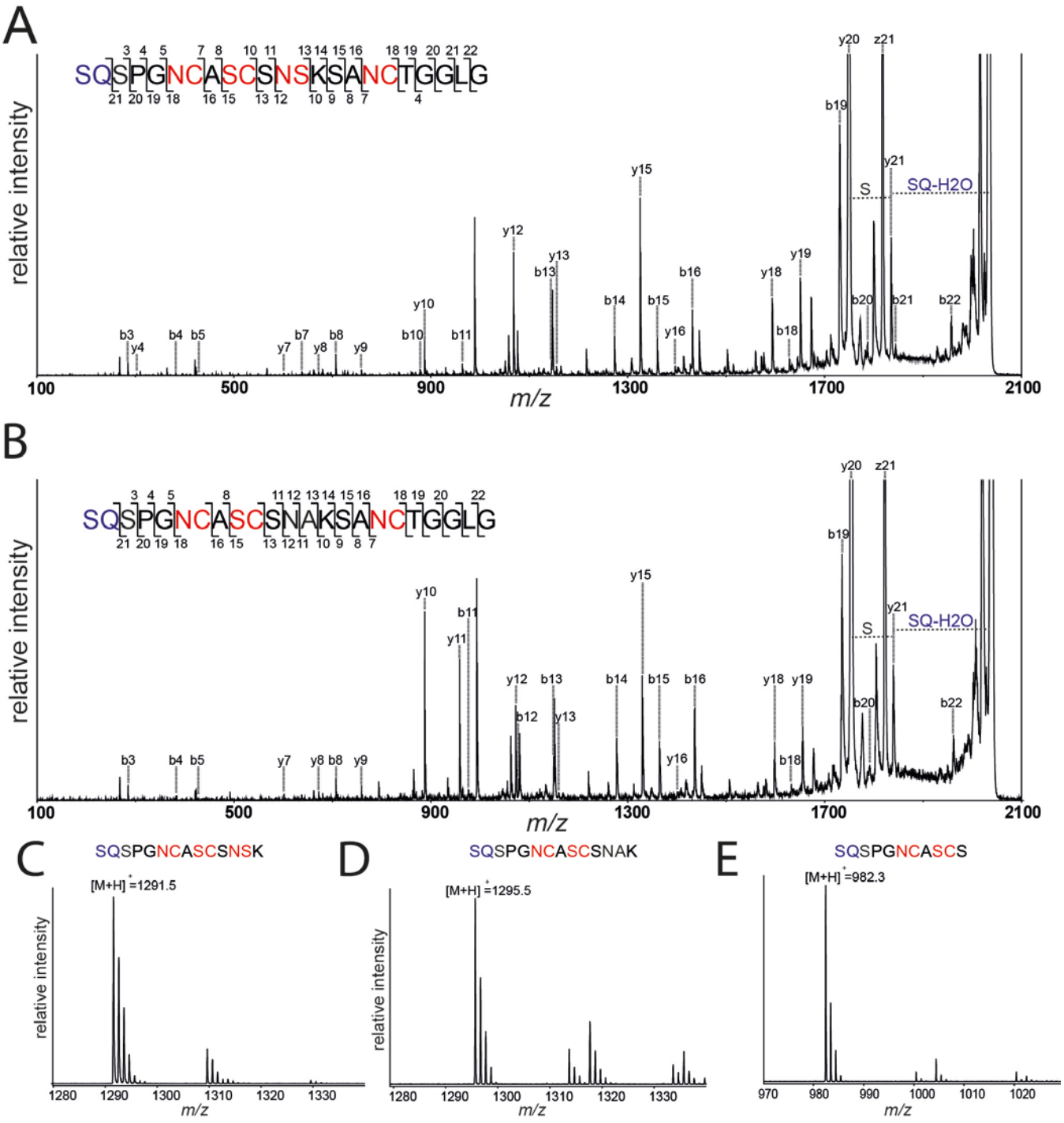

Supplementary Figure 10 | MS/MS fragmentation spectrum of KLB^{A14K} and KLB$^{S13A-A14K}$. An *m/z* scan of purified KLB^{A14K} (**a**) and KLB$^{S13A-A14K}$ (**b**) mutants resulted in ion consistent with the calculated *m/z* for derivatives with amidine ring. The ions were fragmented and produced represented spectra. Diagrams with the observed *b*- and *y*-ions labeled in the structure and in the spectra. (**c**) MALDI-TOF-MS spectra of HPLC purified KLB^{A14K}(1-14) fragment, product of proteolysis of KLB^{A14K} by trypsin. (**d**)

MALDI-TOF-MS spectra of HPLC purified $KLB^{S13A-A14K}$ (1-14) fragment, product of proteolysis of $KLB^{S13A-A14K}$ by trypsin. (**e**) MALDI-TOF-MS spectra of HPLC purified $KLB^{S13A-A14K}$(1-14) fragment, product of proteolysis of $KLB^{S13A-A14K}$(1-14) by carboxypeptidase Y.

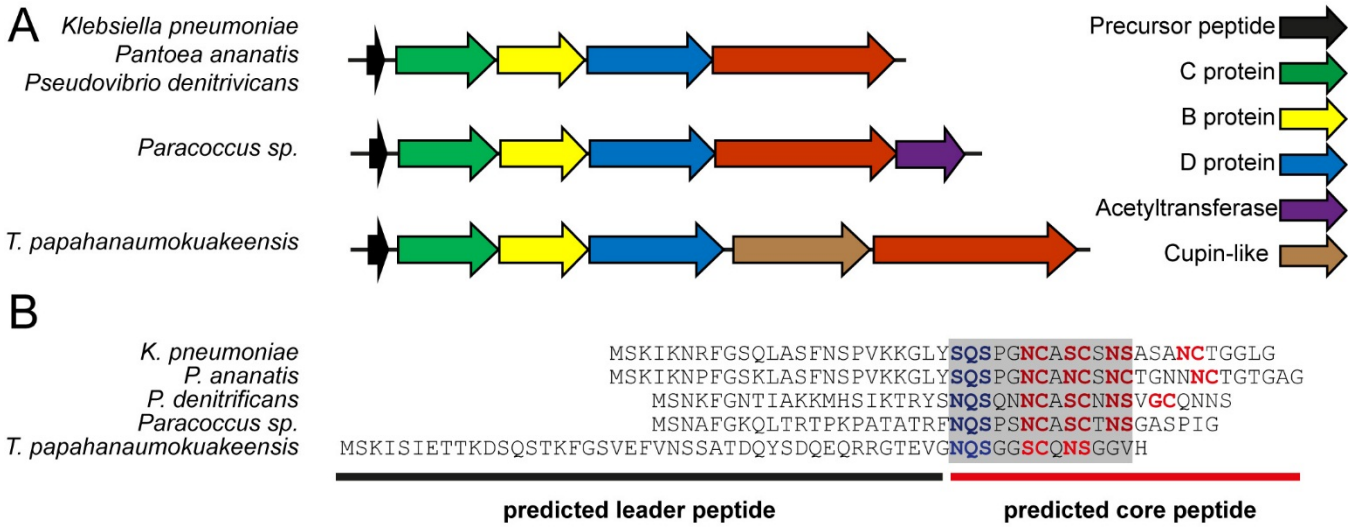

Supplementary Figure 11 | Biosynthetic gene clusters similar to klebsazolicin. (**a**) Schematic representation of gene clusters from *Pantoea ananatis* strain PA4 (JMJK01000000), *Pseudovibrio denitrificans* JCM 12308 (BAZK01000000), *Paracoccus* sp. 228 (JYGY01000000) and *Paracoccus* sp. S4493 (JXYF01000000), and *Terasakiispira papahanaumokuakeensis* strain PH27A (MDTQ01000000) similar to *klpABCDE* gene cluster. (**b**) Alignment of predicted precursor peptides. Predicted residues involved in formation of the amidine ring and azoles are labelled in blue and red, respectively. Conservative part is highlighted by grey rectangle.

II. SUPPLEMENTARY MOVIE

Supplementary Movie 1 | KLB functional site in the 70S ribosome. The movie shows: (1) zoom-out and (2) close-up views of the KLB binding site in the large subunit of the *T. thermophilus* 70S ribosome programmed with mRNA and three tRNAs; (3) details of KLB interactions with the 23S rRNA in the PTC of the ribosome; (4) occlusion of the nascent peptide exit tunnel by KLB molecule.

III. SUPPLEMENTARY DATASETS

Supplementary Dataset 1 | Raw data for the luciferase luminescence assay shown in Figure 2b. Inhibition of protein synthesis by increasing concentrations of KLB in the *in vitro* cell-free translation in S30 extract. Efficiency of protein synthesis is measured in arbitrary luciferase luminescence units. Data for three independent measurements at each given concentration of KLB are shown. Each data point on the plot represents the average of three independent measurements. Standard deviations for each data point are calculated, however, the error-bars are not shown on the plot due to their small size.

IV. SUPPLEMENTARY TABLES

Supplementary Table 1 | NMR chemical shift assignments for amino acid residues in klebsazolicin (DMSO-d6).

		HN	N	CA	C“	HA	CB	HB1	HB2	C	CD	HD	CG	HG
Ser	1			60.625	169.22	3.785	63.673	3.630	3.524					
Ser	1’	7.942		54.296	171.270	4.588	61.815	3.346	3.346					
Gln	2	7.953	116.778	52.009	156.856	3.948	30.450	2.108	1.862		30.352	2.096, 1.948	173.53	
Gln	2’	7.920	117.315	51.700	155.780	3.942	32.609	1.996	1.885		30.650	2.230, 2.000	174.32	
Ser	3	7.925		54.298	170.990	4.680	61.790	3.346	3.346					
Ser	3’			58.040	170.70	3.724	63.693	3.622	3.603					
Pro	4			59.907	171.740	4.346	28.836	2.054	1.896		24.209	1.939, 1.859	46.942	3.923
Gly	5	7.982	104.990	41.938	168.572	3.726								
Asn	6	8.38	121.138	48.08	170.781	5.473	39.37	2.926	2.733	172.573				
Asn	6’	8.35	121.138	48.08	170.781	5.473	39.26	2.926	2.733	172.573				
Ala	8	8.065	117.830	47.955	172.148	4.678	18.670	1.418						
Ser	9	8.851	118.199	53.718	171.641	5.188	62.906	3.890	3.845					
Ser	11	8.017	110.802	54.582	169.24	4.531	61.731	3.730	3.690					
Asn	12	8.68	118.138	44.06	163.164	5.37	37.69	2.91	2.70	170.448				
Ala	14	7.847	118.441	47.835	171.796	4.558	18.631	1.339						
Ser	15	8.119	112.423	54.790	169.53	4.375	61.651	3.658	3.605					
Ala	16	8.000	120.737	48.216	171.799	4.341	17.825	1.285						
Asn	17	8.63	120.341	48.28	170.595	5.483	39.36	2.922	2.710	173.008				
Thr	19	7.941	108.719	58.105	170.061	4.421	66.525	4.156	-	-	19.665	1.099		
Gly	20	8.236	107.130	42.236	168.958	3.792								
Gly	21	7.977	103.143	41.916	168.308	3.767								
Leu	22	7.831	117.724	50.884	171.800	4.325	40.793	1.475	1.513		23.982	1.612	21.450 22.825	0.839 0.873
Gly	23	7.929	106.090	41.020	171.863	3.680								
		C5	**H5**	**C2**	**C4**	**C6**								
Thz	7	123.949	8.174	170.781 SH	148.539	159.628								
Thz	10	124.215	8.184	171.641	148.994	159.908								
Oxz	13	141.667	8.512	163.164 SH	135.370	159.137								
Thz	18	124.258	8.190	170.595 SH	148.639	160.250								

Supplementary Table 2 | Klebsazolicin MICs for various *E. coli* rRNA mutant strains.

Strain (mutation)	MIC, μg/ml	MIC, μM	Fold change
SQ110DTC[a] (pBAD-*sbmA-ompF)*	64	32	1
SQ110DTC (pBAD-*sbmA-ompF)* (*rrsX* U2609G)[b]	256	130	4
SQ110DTC (pBAD-*sbmA-ompF)* (*rrsX* U2609A)[b]	256	130	4
SQ171DTC[c]	128	65	1
SQ171DTC (*rrsX* A2058G)[d]	512	259	4
SQ171DTC (*rrsX* A2058U)[d]	512	259	4
SQ171DTC (*rrsX* A2059C)[d]	512	259	4
SQ171DTC (*rrsX* A2059G)[d]	1024	519	8
SQ171DTC (*rrsX* A2059U)[d]	256	130	2
SQ171DTC (*rrsX* U2584C)[d]	1024	519	8
SQ171DTC (*rrsX* U2609A)[d]	512	259	4
SQ171DTC (*rrsX* U2609C)[d]	128	65	1
SQ171DTC (*rrsX* U2609G)[d]	1024	519	8

[a] MG1655 Δ*tolC*, Δ(*rrnA, rrnB, rrnC, rrnD, rrnG, rrnH*)
[b] Spontaneous resistance mutations
[c] MG1655 Δ*tolC*, Δ(*rrnA, rrnB, rrnC, rrnD, rrnE, rrnG, rrnH*), pAM552
[d] Engineered resistance mutations

Supplementary Table 3 | Nucleotide sequences of primers used for cloning and Sanger sequencing verification.

Name	Primer (5'-3')	Purpose
klpcF	ATTATGAGCTCAAATAACATTTATAAGGCCGCAG	Molecular cloning of *klpBCDE*
klpeR	ATTATCTGCAGCTTAAAAATTATTTAATTCCATTACAACAT	
klpaF	ATAATCCATGGCTAAAATCAAGAATCGTTTTGG	Molecular cloning of *klpA*
klpaR	ATTATCTCGAGTTAACCTAAGCCACCTGTACAATTA	
klpaR2	ATTATGAGCTCTTAACCTAAGCCACCTGTACAATTA	Molecular cloning of *klpA2*
klpaS3A	ATTATCTCGAGTTAACCTAAGCCACCTGTACAATTAGCACTGGCACT ATTTGAACAACTTGCACAATTACCCGGTGCCTGACTATAGAGTCCCT TCTT	Molecular cloning for preparation of KlpA Ser3Ala mutant
klpaQ2N	ATTATCTCGAGTTAACCTAAGCCACCTGTACAATTAGCACTGGCACT ATTTGAACAACTTGCACAATTACCCGGTGAGTTACTATAGAGTCCCT TCTT	Molecular cloning for preparation of KlpA Gln2Asn mutant
klpaS1A	ATTATCTCGAGTTAACCTAAGCCACCTGTACAATTAGCACTGGCACT ATTTGAACAACTTGCACAATTACCCGGTGACTGAGCATAGAGTCCCT TCTT	Molecular cloning for preparation of KlpA Ser1Ala mutant
klpaA14K	ATTATCTCGAGTTAACCTAAGCCACCTGTACAATTAGCACTTTTACT ATTTGAACAACTTGCACAA	Molecular cloning for preparation of KlpA Ala14Lys mutant
klpaA11K	ATTATCTCGAGTTAACCTAAGCCACCTGTACAATTAGCACTGGCACT ATTTTTACAACTTGCACAATTACCCG	Molecular cloning for preparation of KlpA Ala11Lys mutant
klpaS13AA14K	ATTATCTCGAGTTAACCTAAGCCACCTGTACAATTAGCACTTTTCGC ATTTGAACAACTTGCACAATT	Molecular cloning for preparation of KlpA Ser13Ala-Ala11Lys mutant
sbmaF	ATTAACCATGGTTAAGTCTTTTTTCCCAAAG	Molecular cloning of *sbmA*
sbmaR	TAATTGGATCCTTAGCTCAAGGTATGGGTTACTTC	
ompfF	TAATTCATATGATGAAGCGCAATATTCTGGC	Molecular cloning of *ompF*
ompfR	TAATTCTCGAGTTAGAACTGGTAAACGATACCCAC	
klpeF	ATTATCCATGGAAAAGATTCTATACATTGCATC	Molecular cloning of *klpE*
klpeR2	ATTATGAGCTCCTTAAAAATTATTTAATTCCATTACAACAT	
rrnE1	GGATTTGACTATTACAGAG	Sequencing of *rrnE* gene
rrnE2	AAATTGAAGAGTTTGATCATG	
rrnE3	CTGTCGTCAGCTCGTGTTGTG	
rrnE4r	AATGGCGCATACAAAGAGAAGC	
rrnE5	GGTTAAGCGACTAAGCGTAC	
rrnE6	CGGCGGGTGCTAACGTCCGTCG	
rrnE7	GCGAAATTCCTTGTCGGGTAA	
rrnE8r	GGATAGGTGGGAGGCTTTGAAGT	
rrnE9	AGCTGGGTTTAGAACGTCGTG	
rrnE10	GGTTAAGCGACTAAGCGTAC	
rrnE11	CACTAACTGGAGGACCGAAC	
rrnE12r	GCGAAATTCCTTGTCGGGTAA	
rrnE13	GGATAGGTGGGAGGCTTTGAAGT	
rrnE14r	CCTTACAACGCCGAAGGTGTTT	
U2584C-1	CTTAGAACGTCGTGAGACA	Site mutagenesis of pAM552 plasmid at position U2584
U2584C-2	CCAGCTCGCGTACCACTT	

Supplementary Table 4 | Data collection and refinement statistics.

	70S-KLB with A-, P- and E-tRNAs
Data collection	
Space group	$P2_12_12_1$
Cell dimensions	
a, *b*, *c* (Å)	209.64, 449.06, 622.01
α, β, γ (°)	90.0, 90.0, 90.0
Resolution (Å)	364-2.70 (2.77-2.70)[a]
R_{merge}	15.9 (137.7)
$I / \sigma I$	9.20 (0.97)[b]
Completeness (%)	99.3 (93.0)
Redundancy	4.97 (3.60)
Refinement	
Resolution (Å)	2.70
No. reflections	1,572,843
R_{work} / R_{free}	20.7/25.2
No. atoms	
Protein	90,976
Ligand/ion	203,179
Water	5,861
B factors	
Protein	55.5
Ligand/ion	52.5
Water	40.5
r.m.s. deviations	
Bond lengths (Å)	0.005
Bond angles (°)	0.888

Values in parentheses are for highest-resolution shell.

[a] Single crystal was used to obtain the structure

[b] I/σI = 2 at 2.87Å resolution

V. SUPPLEMENTARY REFERENCES

1. Polikanov, Y.S., Steitz, T.A. & Innis, C.A. A proton wire to couple aminoacyl-tRNA accommodation and peptide-bond formation on the ribosome. *Nat. Struct. Mol. Biol.* **21**, 787-793 (2014).

2. Bulkley, D., Innis, C.A., Blaha, G. & Steitz, T.A. Revisiting the structures of several antibiotics bound to the bacterial ribosome. *Proc. Natl. Acad. Sci. USA* **107**, 17158-17163 (2010).

3. Noeske, J. et al. Synergy of streptogramin antibiotics occurs independently of their effects on translation. *Antimicrob. Agents. Chemother.* **58**, 5269-5279 (2014).

4. Gagnon, M.G. et al. Structures of proline-rich peptides bound to the ribosome reveal a common mechanism of protein synthesis inhibition. *Nucleic Acids Research* **44**, 2439-2450 (2016).

5. Roy, R.N., Lomakin, I.B., Gagnon, M.G. & Steitz, T.A. The mechanism of inhibition of protein synthesis by the proline-rich peptide oncocin. *Nat. Struct. Mol. Biol.* **22**, 466-469 (2015).